Control Design for a Floating Wind Turbine
Assignment Part II
SC42145 Robust Control

Long Youyuan, 5690641
Qingyi Ren, 5684803
Delft University of Technology

January 20, 2023

1 Introduction

In this assignment, we are given the a floating wind turbine system in Fig 1 and required to investigate the controller design methods. Firstly, the floating wind turbine system is nonlinear one, for better analysis, the linearisation is performed at the wind speed $V_{in} = 14m/s$ to obtain linear state-space model:

Figure 1: An example of a Floating Wind Turbine (FWT).

$$\dot{x} = Ax + Bu \tag{1}$$
$$y = Cx + Du \tag{2}$$

where $x \in \Re^{5\times1}$, $A \in \Re^{5\times5}$, $B \in \Re^{5\times3}$, $u \in \Re^{3\times1}$,$y \in \Re^{2\times1}$, $C \in \Re^{2\times5}$ and $D \in \Re^{2\times3}$. The state vector, input and output of the linearized system are defined as $x = [x_1; x_2; x_3; x_4; x_5]$, $u = [\beta; \tau_e; V]$ and $y = [w_r; z;]$, and matrices A, B, C and D are given in MATLAB file. Secondly, the model has three inputs, which is stacked in the vector u, including blade pitch angle β [rad], the generator torque τ_e $[N \cdot m]$ and the wind speed V [m/s] which is the derivation from from the linearisation point (β and τ_e are the control inputs of system and V is the disturbance input of the system). Then generator speed w_r [rad/s] and the fore-aft tower top displacement Z [m] are taken as the output of the system, which composing the output vector y. Finally the fore-aft tower top displacement Z can be decomposed as $Z = Z_1 + Z_2$ where Z_1 and Z_2 represent tower bending and platform tilting modes respectively, shown in Fig 2. The state vector $x = [x_1; x_2; x_3; x_4; x_5]$ describes dynamics of the system $x_1 = w_r$, $x_2 = \dot{z_1}$, $x_3 = z_1$, $x_4 = \dot{z_2}$ and $x_5 = z_2$.

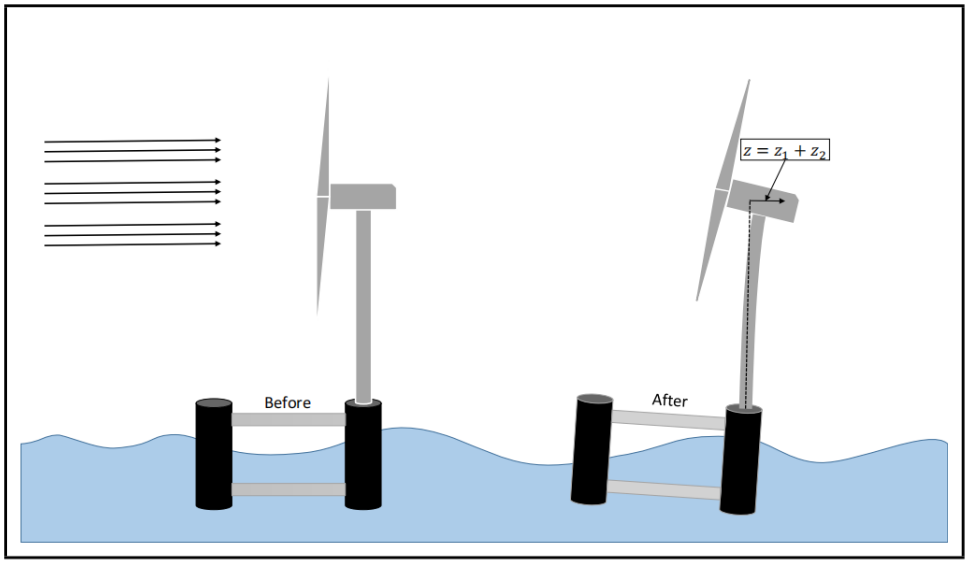

Figure 2: Schematic depiction of fore-aft movement.

As former assignment, the MIMO weighting design based on controller sensitivity function (KS) and sensitivity function (S) is already designed, the plant P has two-dimensional exogenous inputs

w and four-dimensional outputs $\begin{bmatrix} z_1 \\ z_2 \end{bmatrix}$. The performance weights W_p and W_u are defined as

$$W_p = \begin{bmatrix} W_{p11} & 0 \\ 0 & 0.2 \end{bmatrix} \tag{3}$$

$$W_{p11} = \frac{\frac{s}{3} + 0.3 \times 2\pi}{s + 0.3 \times 2\pi \times 10^{-4}} \tag{4}$$

$$W_u = \begin{bmatrix} 0.01 & 0 \\ 0 & \frac{0.005s^2+0.0007s+5\times10^{-5}}{s^2+0.0014s+1\times10^{-6}} \end{bmatrix} \tag{5}$$

, from which the performance signals z_1 and z_2 comes out respectively.

The obtained mixed-sensitivity controller is saved as '**K_last.mat**', which will be used in the following sections to analyse Robust Stability (RS) and Robust Performance (RP) and robust controller design.

2 Analysis of Robust Stability (RS) and Robust Performance (RP)

In this section, the perturbed mixed uncertainty model of floating wind turbine is constructed with the analysis of robustness. The perturbations are defined as Δ. In this assignment, the input and output uncertainty are added to the nominal model between the inputs β and τ_e and the outputs w_r and z respectively.

2.1 Block diagram

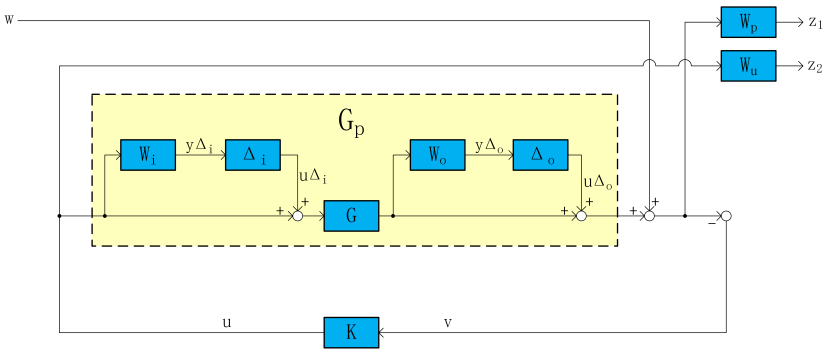

Figure 3: Block diagram of the generalized plant

The block diagram is shown above. In this model,

(1) ω is a 2-dimension exogenous input.

(2) u, v are input signal and output signal of controller respectively and they are both 2-dimension..

(3) $y\triangle_i$ and $y\triangle_o$ are input signals of input and output perturbation block respectively.

(4) $u\triangle_i$ and $u\triangle_o$ are output signals of input and output perturbation block respectively.

(5) z_1, z_2 are both 2-dimension exogenous outputs.

2.2 Mathematical expression for the generalised plant

From figure 3, we can get following equations of generalized plant:

$$\begin{aligned} y_{\triangle i} &= W_i u \\ y_{\triangle o} &= W_o G u_{\triangle i} + W_o G u \\ z_1 &= W_p G u_{\triangle i} + W_p u_{\triangle o} + W_p w + W_p G u \\ z_2 &= W_u u \\ v &= -G u_{\triangle i} - u_{\triangle o} - w - G u \end{aligned} \tag{6}$$

The generalized plant P from input $[u_{\triangle i}, u_{\triangle o}, w, u]^T$ to output $[y_{\triangle i}, y_{\triangle o}, z_1, z_2, v]^T$ is defined as:

$$P = \begin{bmatrix} 0 & 0 & 0 & W_i \\ W_o G & 0 & 0 & W_o G \\ W_p G & W_p & W_p & W_p G \\ 0 & 0 & 0 & W_u \\ -G & -I_{2\times 2} & -I_{2\times 2} & -G \end{bmatrix} \tag{7}$$

2.3 Uncertainty weights and transfer matrix

2.3.1 Frequency response of uncertainty weights

The 2-dimensional input channel uncertainty are decoupled, so it can be seen as two independent SISO uncertainty channels. This is a multiplicative uncertainty, so the magnitude of the frequency response of W_{i1} represents the uncertainty degree. From the figure below, it is noticeable that the uncertainty increases with frequency

and the uncertainty of input channel keeps about 30% when the frequency is less than 10 rad/s. At frequency 50 rad/s, the uncertainty reaches 100%, which means tight control is not possible since this frequency. The magnitude of the curve rapidly increases since frequency is larger than 10 rad/s and arrives at its peak 4 when the frequency is about 1000 rad/s and remains at this value.

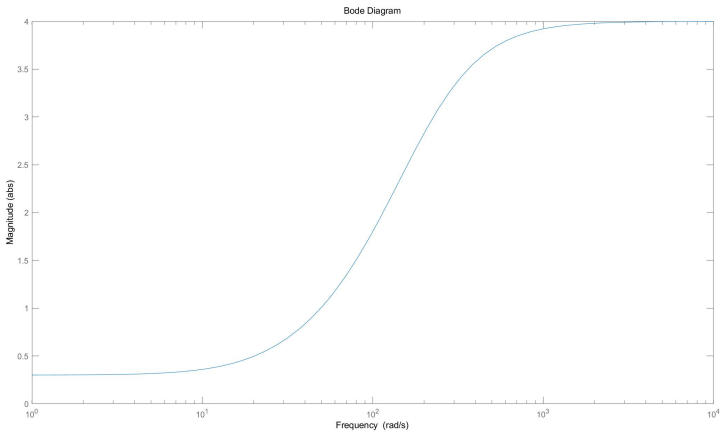

Figure 4: Frequency response of W_{i1}.

From the figure 5, it is clear that the output channel has less uncertainty at low frequency and larger frequency at high frequency than the previous one, but basically, they shows similar property. The uncertainty also ascents with frequency and keeps at its bottom when frequency is less than 1 rad/s. When the frequency is larger than 1 rad/s, the uncertainty starts to surge and reach 1 at frequency around 20 rad/s, which means 100% uncertainty. At around 1000 rad/s, the uncertainty reaches its maximum value, 500%.

2.3.2 Derivation of uncertainty weights

The most possible way to derive the uncertainty weights is by using unmodelled dynamics uncertainty which is a simple multiplicative weight of the form at each input and output channel:

$$w_I(s) = \frac{\tau s + r_0}{\frac{\tau}{r_\infty} s + 1} \tag{8}$$

where r_0 is the relative uncertainty at steady-state, $1/\tau$ is about the frequency where the relative uncertainty arrives at 100%, and

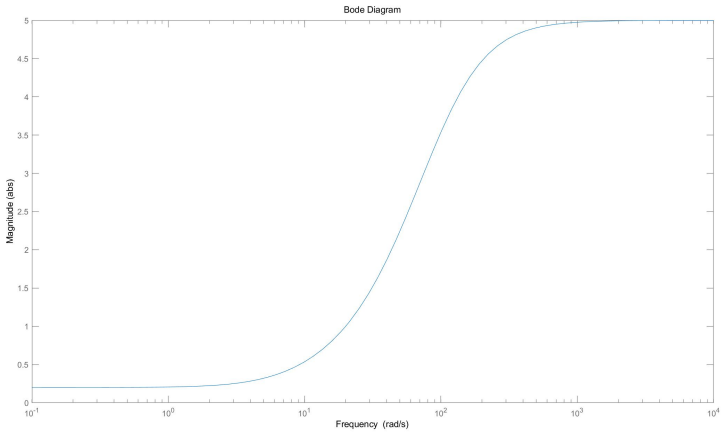

Figure 5: Frequency response of W_{o1}.

r_∞ is the magnitude of the weight at higher frequencies. The input and output uncertainty are always present in a real system, and the input uncertainty usually comes from amplifier dynamics or signal converter, while the output uncertainty comes from the sensors, etc. And in fact, these uncertainty should be considered as diagonal because of the independent scalar uncertainty in each input channel. If it is assumed that the input and output uncertainty are full, then the set of all possible perturbed models will be large and it will result in conservative conclusion.

2.3.3 Singular values of the uncertain transfer matrix

The uncertain transfer matrix is

$$G_p(s) = \Delta_o W_o G(s) \Delta_i W_i \tag{9}$$

With fixed frequency w_0, the uncertain transfer matrix $G_p(s)$ can be decomposed in the form of:

$$G_p(w_0) = U \Sigma V^H \tag{10}$$

where $\Sigma \in 2 \times 2$, $U \in 2 \times 2$ and $V \in 2 \times 2$, U and V are unitary matrices. For V is unitary matrix, the 10 can be written as:

$$\begin{aligned} &G_p(w_0) V = U \Sigma \\ &G_p(w_0) \begin{bmatrix} v_1 & v_2 \end{bmatrix} = \begin{bmatrix} u_1 & u_2 \end{bmatrix} \begin{bmatrix} \sigma_1 & 0 \\ 0 & \sigma_2 \end{bmatrix} \end{aligned} \tag{11}$$

The maximum gain $\bar{\sigma}(G)$ can be obtained by $\max_{v\neq 0} \frac{\|G_P \cdot v\|_2}{\|v\|_2}$. The $\Sigma = \begin{bmatrix} \sigma_1 & 0 \\ 0 & \sigma_2 \end{bmatrix}$ is a square diagonal matrix with the singular values σ_1 and σ_2 on the diagonal. For different frequency w_o, the singular values have different values as $\sigma_1(w_o)$ and $\sigma_2(w_o)$, which are plotted frequency domain in figure (6).

From the figure (6), it is noticeable that the singular values σ_1 and σ_2 cluster get closer at low frequencies and get loose at high frequencies. This is because the input and output uncertainty weight has low magnitude at low frequencies, so the system has smaller set of all possible perturbed models at low frequencies and the singular values of the perturbed models will not deviate much from that of the nominal model. By contrary, when the frequency increase, the uncertainty of the model also increases and in this case, the singular value of perturbed model has more possibility to get more difference with the corresponding one of the nominal model. Therefore, the singular value clusters get looser with frequency.

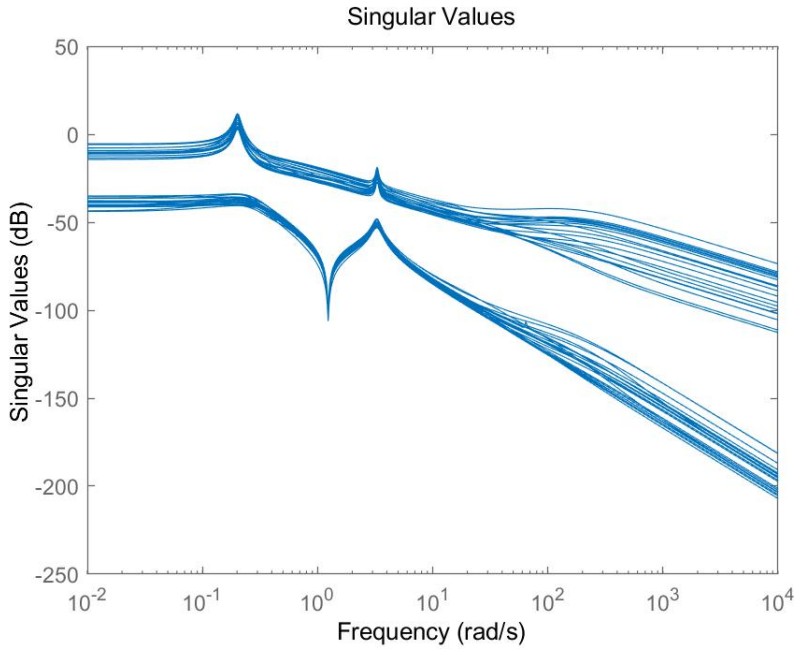

Figure 6: Singular values of the uncertain transfer matrix.

2.4 Performance of formulated generalized system with mixed-sensitivity controller

The generalized system with mixed-sensitivity controller is constructed in MATLAB according to figure (3). The code is showed as

```
systemnames = 'G Wp Wu Wi Wo';
inputvar = '[udeli(2); udelo(2); w(2); u(2)]';
outputvar='[Wi; Wo; Wp; Wu; -G-udelo-w]';
input_to_G = '[u+udeli]';
input_to_Wp = '[G+udelo+w]';
input_to_Wu = '[u]';
input_to_Wi = '[u]';
input_to_Wo = '[G]';
sysoutname='P'; cleanupsysic= 'yes'; sysic;
```

In the uncertainty block diagram in figure (3), all the uncertainties are put in the block Δ,

$$\Delta = \begin{bmatrix} \Delta_i & 0 \\ 0 & \Delta_o \end{bmatrix} \tag{12}$$

where $\Delta_i = \begin{bmatrix} \delta_{i1} & 0 \\ 0 & \delta_{i2} \end{bmatrix}$, $\Delta_o = \begin{bmatrix} \delta_{o1} & 0 \\ 0 & \delta_{o2} \end{bmatrix}$, K represents the mixed-sensitivity controller saved as '**K_last.mat**', P represents plant, Δ_y and Δ_y represent the input and output to the uncertainty block Δ. In generalized case, the mixed-sensitivity controller and the plant can be combined as block N, only having the uncertainty block Δ outside, shown in figure (8). The structure of generalized uncertainty block diagram is shown as:

$$\begin{bmatrix} \Delta_y \\ z \end{bmatrix} = N \begin{bmatrix} \Delta_u \\ w \end{bmatrix} = \begin{bmatrix} N_{11} & N_{12} \\ N_{21} & N_{22} \end{bmatrix} \begin{bmatrix} \Delta_u \\ w \end{bmatrix} \tag{13}$$

The condition that N is internally stable which required the real parts of all the eigenvalue of N are less than zero to check the Nominal Stability(NS) and the μ-conditions to check Nominal Performance(NP), Robust Stability(RS) and Robust Performance(RP) is shown as below:

(1) **NS**: N is internally stable which required the real parts of all the eigenvalue of N are less than zero.

(2) **NP**: $\bar{\sigma}(N_{22}) = \mu_{\Delta_p} < 1$, $\forall w$, and **NS**.

(3) **RS**: $\mu_{\Delta}(N_{11}) < 1$, $\forall w$, and **NS**.

(4) **RP**: $\mu_{\hat{\Delta}}(N) < 1, \forall w$, $\hat{\Delta} = \begin{bmatrix} \Delta & 0 \\ 0 & \Delta_P \end{bmatrix}$ and **NS**.

In MATLAB, the code is shown as below:

```
N=lft(P,K_pre);
max(real(eig(N))) %NS

omega=logspace(-3,3,61);
Nf=frd(N,omega);
blk=[2 4];
[mubnds,muinfo]=mussv(Nf(5:8,5:6),blk,'c');
muNP=mubnds(:,1);
[muNPinf, muNPw]=norm(muNP,inf);
muNPinf  %NP

blk=[1 1;1 1;1 1;1 1];
[mubnds,muinfo]=mussv(Nf(1:4,1:4),blk,'c');
muRS=mubnds(:,1);
[muRSinf, muRSw]=norm(muRS,inf);
muRSinf  %RS

blk=[1 1;1 1;1 1;1 1;2 4];
[mubnds,muinfo]=mussv(Nf(1:8,1:6),blk,'c');
muRP=mubnds(:,1);
[muRPinf, muRPw]=norm(muRP,inf);
muRPinf  %RP
```

In table 1, it shows RP-condition is not satisfied. NS-condition, NP-condition and NS-condition are satisfied with the conditions that all real parts of eigenvalues of matrix N are negative, $\bar{\sigma}(N_{22}) = \mu_{\Delta_p} < 1, \forall w$, and $\mu_{\Delta}(N_{11}) < 1, \forall w$ respectively. The obtained condition of **NS** that all real parts of eigenvalues of matrix N are negative is satisfied because the maximum real part of eigenvalues of matrix N is less than 0, which means there are no non-stable poles in transfer function N.

It is worth mentioning that the MATLAB function **minreal(N)** (minimal realization) is vital and necessary for this assignment. For our initial experiment, the maximum real part of eigenvalues of the transfer function N was a positive value as 0.0221, however when looking at the nyquist plots in figure (9), we found a contradiction that all the MIMO system was stable based on the analysis of nyquist plot of each input and output. To solve the problem, the **pole** and **zero** functions were employed to obtain the poles and zeros of transfer function N, it was observed that there were the same number of zeros and poles of the same positive value 0.0221. After applying **minreal(N)** to remove 56 states, the **NS** condition

is satisfied and the nyquist plots help to verify it.

$$det(I + L(s)) = c \cdot \frac{Closed\ Lp\ characteristic\ polynomial}{Open\ Lp\ characteristic\ polynomial} \quad (14)$$

To check the internally stability of the system, generalized Nyquist method is used here. Firstly, figure (9) is the Nyquist plot of transfer function $det(I - L(s))$, where the $L(s)$ the the open loop transfer function of the system, which is equal to $G(s) * K_p re(s)$. When zooming in this plot at $(-1, 0j)$ point, the figure (10) is acquired. From figure (10), it is concluded that the contour map of $det(I - L(s))$ encircles origin **2** times anti-clockwise.

Secondly, it can be calculated that the open-loop transfer function $L(s)$ has **two** RHP poles in the right half plane, which are a pair of complex poles $0.0221 \pm 3.5415i$.

By applying formula 14 and Cauchy's argument principle, the equation should be satisfied:

$$N = P - N = 0 \quad (15)$$

where P represents the number of poles of open-loop transfer function $L(s)$ lying on the right half plane and N represents the number of times that the Nyquist graph of the open-loop transfer function $L(s)$ winds counterclockwise about the point $(-1, j0)$. In this case, $P = N = 2$ and $Z = 0$. The conclusion can be reached that there is no unstable closed loop poles of the generalized MIMO system. Therefore, the generalized MIMO system is internally stable, which verifies the condition **NS**.

The obtained μ-condition of RP is 1.2896, which means the RP-requirement would be satisfied if the performance requirement and uncertainty is reduced by a factor of 1.2896 [2].

Check μ-conditions of NS, NP, RS and RP	
Maximum real part of eigenvalue of matrix N (check NS)	-1.8850×10^{-4}
μ of NP	0.6105
μ of RS	0.5442
μ of RP	1.2896

Table 1: Check μ-conditions of NS, NP, RS and RP.

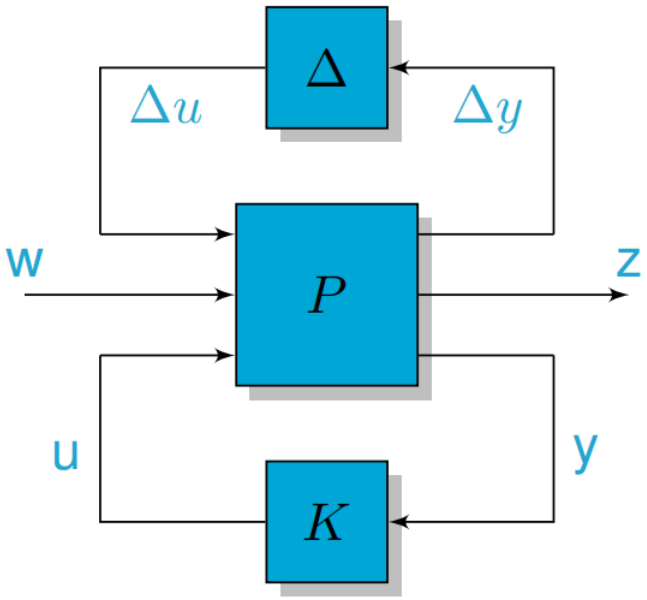

Figure 7: Uncertainty block diagram.

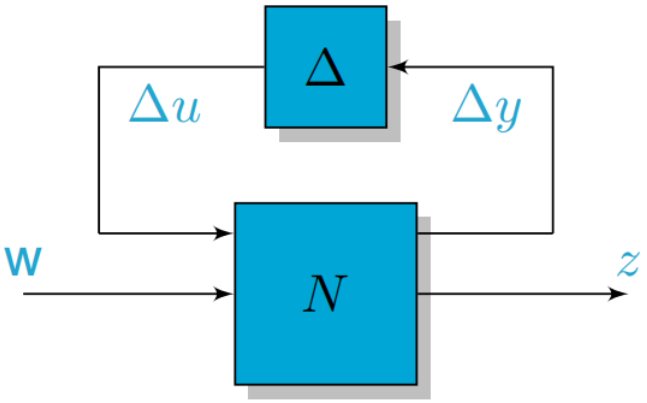

Figure 8: Generalized uncertainty block diagram.

2.5 The relationship of μ-condition for NP and H∞ norm of the objective function

The relationship is shown below:

$$\|N_{22}\|_{\infty} = \max_{w} \bar{\sigma}(N_{22}(jw))) = \mu_{\Delta_p}(N_{22}) \tag{16}$$

where Δ_p is full. The proof is shown as below:

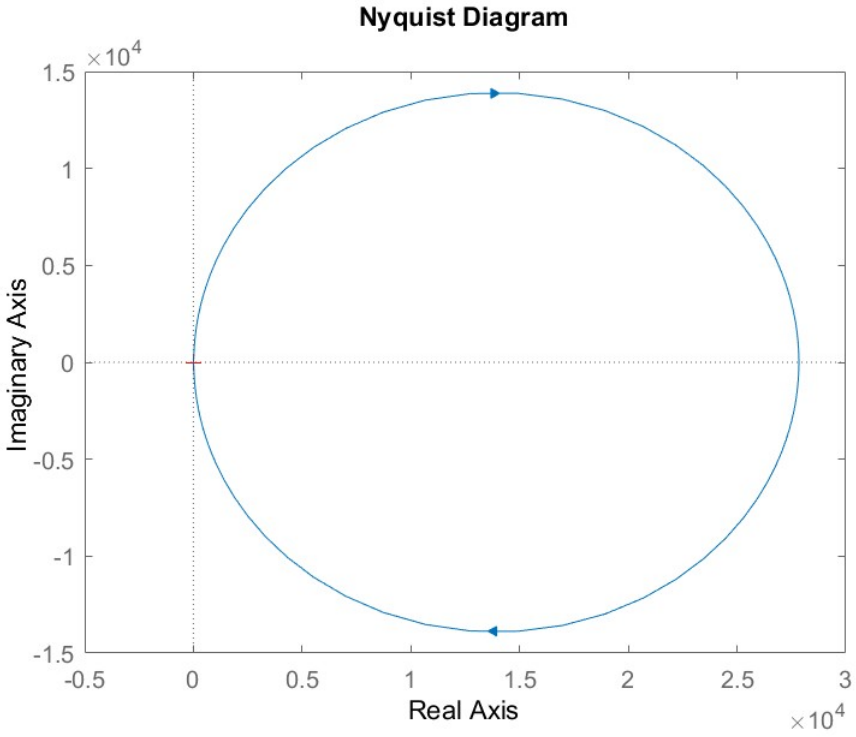

Figure 9: Generalized Nyquist plot of $det(I - L(s))$.

Proof.

$$\frac{1}{\mu_{\Delta_p}(N_{22})} = \min\{k_m | \det(I - k_m N_{22}\Delta_p) = 0 \text{ ,for structured } \sigma(\bar{\Delta}_p) \leq 1\} \tag{17}$$

The definition of μ is shown above. To make $\det(I - k_m N_{22}\Delta_p)=0$, the square matrix $k_m N_{22}\Delta_p$ must has at least one eigenvalue that is equal to 1. Therefore, we get

$$\begin{aligned} \lambda_i(k_m N_{22}\Delta_p) = 1, \ \exists i \\ \Rightarrow k_m = \frac{1}{\lambda_i(N_{22}\Delta_p)}, \ \exists i \end{aligned} \tag{18}$$

To minimize k_m, $\lambda_i(N_{22}\Delta_p)$ should be maximized. Therefore,

$$\begin{aligned} k_m = \frac{1}{\max_{\Delta_p}(\max_\omega \rho(N_{22}\Delta_p))} \\ \Rightarrow \mu_{\Delta_p}(N_{22}) = \frac{1}{k_m} = \max_{\Delta_p}(\max_\omega \rho(N_{22}\Delta_p))) \end{aligned} \tag{19}$$

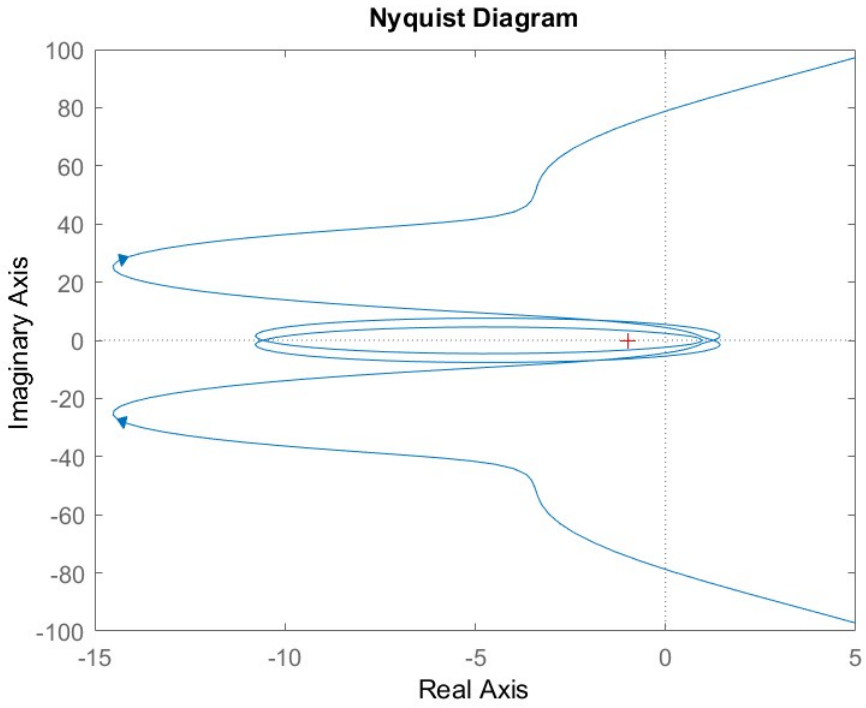

Figure 10: Generalized nyquist plot:Zoom at $(-1, 0j)$.

From Lec 5, slide 13, we know that if Δ_p is full, then

$$\max_{\Delta_p}(\max_{\omega} \rho(N_{22}\Delta_p)) = \max_{w} \bar{\sigma}(N_{22}(jw))) \tag{20}$$

Therefore,

$$\mu_{\Delta_p}(N_{22}) = \max_{w} \bar{\sigma}(N_{22}(jw))) = \|N_{22}\|_{\infty} \tag{21}$$

□

3 Robust Control Design

In this section, the synthesized controller is designed to achieve robust stability (RS) and robust performance (RP) by employing DK iteration procedure.

3.1 Symbolic expression for the D matrices

To check robust performance, one straight way is to check $\bar{\sigma}(N(k))$. However, if the uncertainty block is structured, this method will be

conservative. Therefore, we should introduce D matrices to obtain the least conservative RP condition.

The figure 11 shows the structure of RP with D_1, D_2, where $D_1 D_2 = I_8$, $D_2 D_1 = I_6$ and $D_1 \hat{\Delta} = \hat{\Delta} D_2$, so the whole structure does not change and the new uncertainty block with D_1, D_2 also does not change.

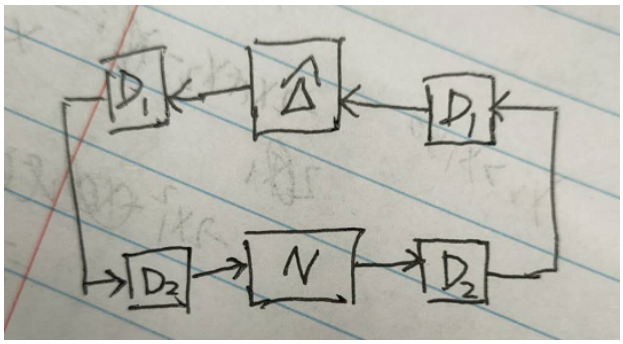

Figure 11: Robust stability structure with D

In this case, $\hat{\Delta} = diag\{\Delta, \Delta_P\}$, where Δ is a 4×4 diagonal complex matrix and Δ_P is a 2×4 full complex matrix. Therefore, D_1 is a 8×6 matrix, D_1 = diag{d1,d2,d3,d4,D11}, where d1 to d4 are saclers and D11 is a 4×2 matrix. While D_2 is a 6×8 matrix, D_2 = diag{1/d1,1/d2,1/d3,1/d4,D22}, where D22 is a 2×4 matrix.

3.2 DK iteration procedure

In the former section, the $\mu-$analysis is applied to analyse the **NP**, **RS** and **RP** of the MIMO system. In order to obtain the optimal controller, μ-synthesis problem is constructed by minimizing a μ condition. It is worth mentioning that there is no direct method to obtain the optimal solution to the controller synthesis problem but it has an upper bound

$$\mu(N(K)) \leq \min_{D} \bar{\sigma}(DN(K)D^{-1}) \tag{22}$$

. Then the optimal controller can be obtained as,

$$\min_{k}(\min_{D} \left\| DN(K)D^{-1} \right\|_{\infty}) \tag{23}$$

The controller can be obtained through minimising $\|DN(K)D^{-1}\|_{\infty}$ by alternately using D and K. The DK iteration can be split into two processes: D-step and K-step. The detailed methods are shown as below:

(1) **D-step**: Synthesis a controller that minimizes the scaled problem, $\min_K \|DN(K)D^{-1}\|_\infty$.

(2) **K-step**: Find $D(jw)$ to minimize $\bar{\sigma}(D(jw)N(jw)D^{-1}(jw))$ at each frequency with the number of frequency points fixed N.

(3) Fit the transfer function on top of $D(jw)$ and return to step 1.

Note that D starts with identity matrix. In MATLAB, **musyn** is used to employ automatic D-K iterations shown in the following MATLAB code,

```
Delta=[ultidyn('D1',[1,1]) 0 0 0; 0 ultidyn('D2'
    ,[1,1]) 0 0; ...
        0 0 ultidyn('D3',[1,1]) 0; 0 0 0 ultidyn('D4'
    ,[1,1])];
Punc=lft(Delta,P);
opts = musynOptions('Display','full','MixedMU','on','
    FullDG',false,'MaxIter',20);
[K,CLperf] = musyn(Punc,2,2,opts);
```

The returned matrix **K** represents the state-space (ss) model of the controller which yields the H_∞ performance, **CLperf** represents a positive scalar which is the best achieved robust performance. The resulting D-K iteration summary is shown as below

```
D-K ITERATION SUMMARY:
------------------------------------------------
Robust performance                    Fit order
------------------------------------------------
  Iter    K Step     Peak MU     D Fit     D
    1     11.65      8.478       8.574     18
    2     4.185      4.092       4.123     20
    3     1.375      1.256       1.262     34
    4     1.021      1.016       1.027     40
    5     0.9889     0.9856      1.148     34
    6     0.9832     0.9826      1.001     38
    7     0.9777     0.9766      0.989     38

Best achieved robust performance: 0.977
```

The number of iteration is 7 and the best achieved robust performance is 0.977 which means that the gain from w to z remains below 0.977 [3], the μ-condition of RP is satisfied. The K Step, Peak MU, D Fit and D in D-K iteration summary have the representations as followed:

(1) K Step: represent the value of H_∞ performance of the closed-loop synthesized system. When the iteration goes on, it repre-

sents the scaled H_∞ performance of renewed closed-loop synthesized system.

(2) Peak MU: robust performance $\bar{\mu}$, which is an upper bound of μ to help to design controller in the **K-step**.

(3) D Fit: scaled H_∞ performance after fitting the D and G rational functions scaling after **K-step**.

(4) Fit order for D: Order of the rational function D used to fit the scaling in the current iteration.

In **musynOptions**, the 'Display' is set to be 'full' to illustrate the details of each iteration including plots of D scaling data and the frequency dependence of absolute value of singular value μ [4]. In figure (12), it compares the robust performances before fitting and after fitting in the last iteration. The line for MU upper bound represents the robust performance before fitting: $\bar{\mu}$, the upper bound of μ, as the function in frequency domain. The line for Scaled CL for D data represents scaled H_∞ performance before fitting the D scaling rational function. In comparison, Scaled CL for fitted D is the scaled H_∞ performance after fitting the D scaling rational function.

Check μ-conditions of NS, NP, RS and RP	
Maximum real part of eigenvalue of matrix N (check NS)	-1.8850×10^{-4}
μ of NP	0.6809
μ of RS	0.5259
μ of RP	0.9751

Table 2: Check μ-conditions of NS, NP, RS and RP.

The value of μ is shown in the table 2. The maximum real part of eigenvalue of matrix N is less than 0, so the system has NS. the value of μ for NP, RS and RP are all less than 1. This means this controller achieves NP, RS and RP at the same time.

3.3 Time-domain simulation and analysis

In order to compare the performance mixed-sensitivity controller with previous MIMO controller, we plug the two controllers to the closed-loop systems respectively and obtain their step responses to compare the control performance.

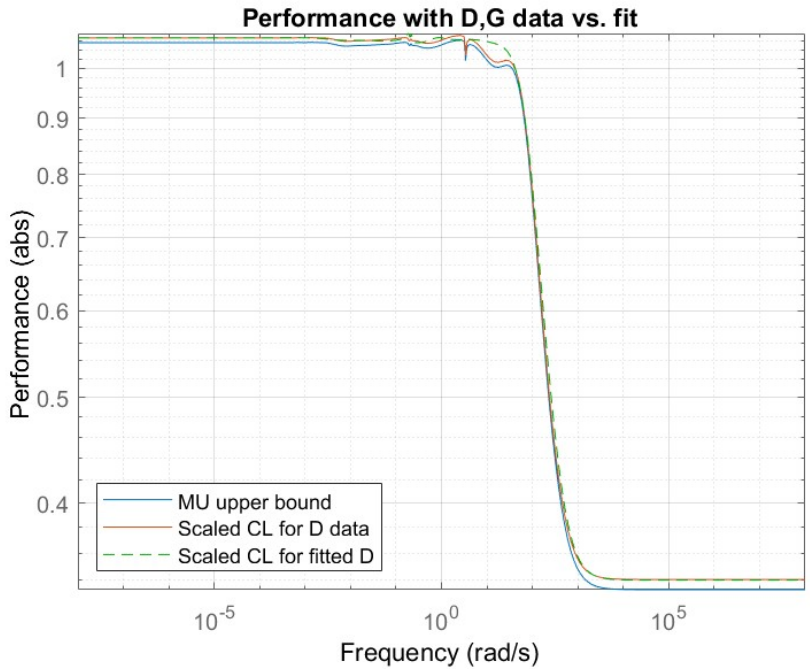

Figure 12: . Robust performances of closed loop system before fitting and after fitting in the last iteration.

```
L1 = G*K_pre;
L2 = G*K;
sys1 = feedback(G,K_pre);
sys2 = feedback(G,K);
figure();
step(sys1,sys2);
legend('previous MIMO controller','mixed-sensitivity
   controller')
```

In figure (13), it shows the step responses of closed-loop system with mixed-sensitivity controller and with previous MIMO controller respectively. Note that the closed-loop system mentioned before is MIMO system, with two inputs β and τ_e and two outputs w and z, the step responses of the system are split into 4 sub pictures, each one shows the step response of one output to one input. For the first sub picture, it depicts the step response of output w to input β, for the closed-loop system with mixed-sensitivity controller, the response has higher overshoot than the system with previous MIMO controller, however it has smaller settling time. The same conclusion applied to the second sub picture, the step response of

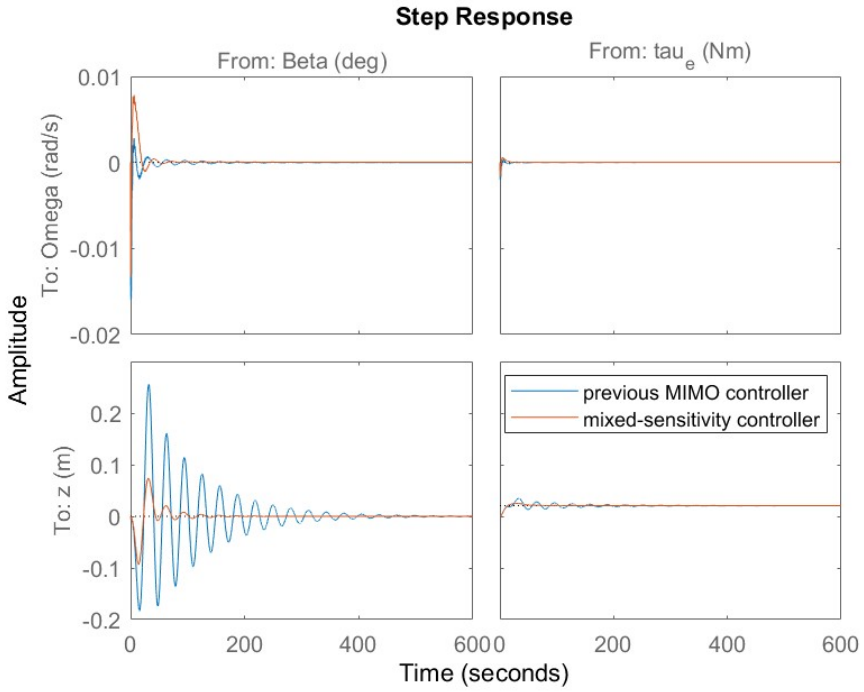

Figure 13: The step responses of closed-loop system with mixed-sensitivity controller and with previous MIMO controller respectively.

output w to input τ_e. For the third and the fourth sub pictures, the step response of closed system with mixed sensitivity controller has smaller overshoot and at the same time have the smaller settling time, which shows that overall the mixed-sensitivity controller has better control performance than the previous MIMO controller.

In order to compare the robustness of the two controllers, inspired by the former experiment with windspeed data mixed with sine wave as input to the system, two closed-loop systems are built with different controller: mixed-sensitivity controller and previous MIMO controller. Two systems' structure implemented two different controllers with weights in the simulink is shown in figure 14, with winddata as output (It combines a low frequent part (a sin wave with a period of around 1000 seconds) and some high-frequency turbulence).

From figures (15) and (16), it can be noticed that the closed-loop system with mixed-sensitivity controller has higher robustness to the windspeed input. More specifically, the mixed-sensitivity

controller can eliminate the high frequency component in the output to large extent, the main part left in the output w_2 is low frequency component and only has slight high frequency wave added to itself, which can be viewed as response to the low frequency component of windspeed (sine wave) input only. However, for closed-loop system with previous MIMO system, the property of robustness to high frequency component in input is relatively worse, there exist evident high frequency wave with larger amplitude in the output w_2, which is added to low frequency output response.

In conclude, the mixed sensitivity controller not only has better control performance (based on smaller overshoot and settling time of step response) and stronger robustness to high frequency turbulence in the windspeed as input to closed-loop system.

In frequency domain, the bode plots of two open-loop systems ($L = P \cdot K$, where L is transfer function of open-loop system, P and K are transfer functions of plant and controller respectively) with mixed sensitivity controller and previous MIMO controller are shown in figure (17). From the bode plots, it can be observed that phase plots of open-loop systems between the first input β and the two outputs w and z almost remain the same, however the margin plots of open-loop systems between the first input β and the two outputs w and z show the difference, the margin plots of open-loop systems with mixed sensitivity controller are higher than those of open-loop systems with previous MIMO controller in low frequency part when $w < 3.62$rad/s, which helps to decrease phase margin.

For the open-loop systems between second input τ_e and the two outputs w and z, the margin plots have the similar characteristics, the margin plots of open-loop systems with mixed sensitivity controller are higher than those of open-loop systems with previous MIMO controller in low frequency part when $w < 3.62$rad/s. For the phase plots, the open-loop systems with mixed sensitivity controller are globally higher than those of open-loop systems with previous MIMO controller, which lead to the decrease in both phase margin and gain margin.

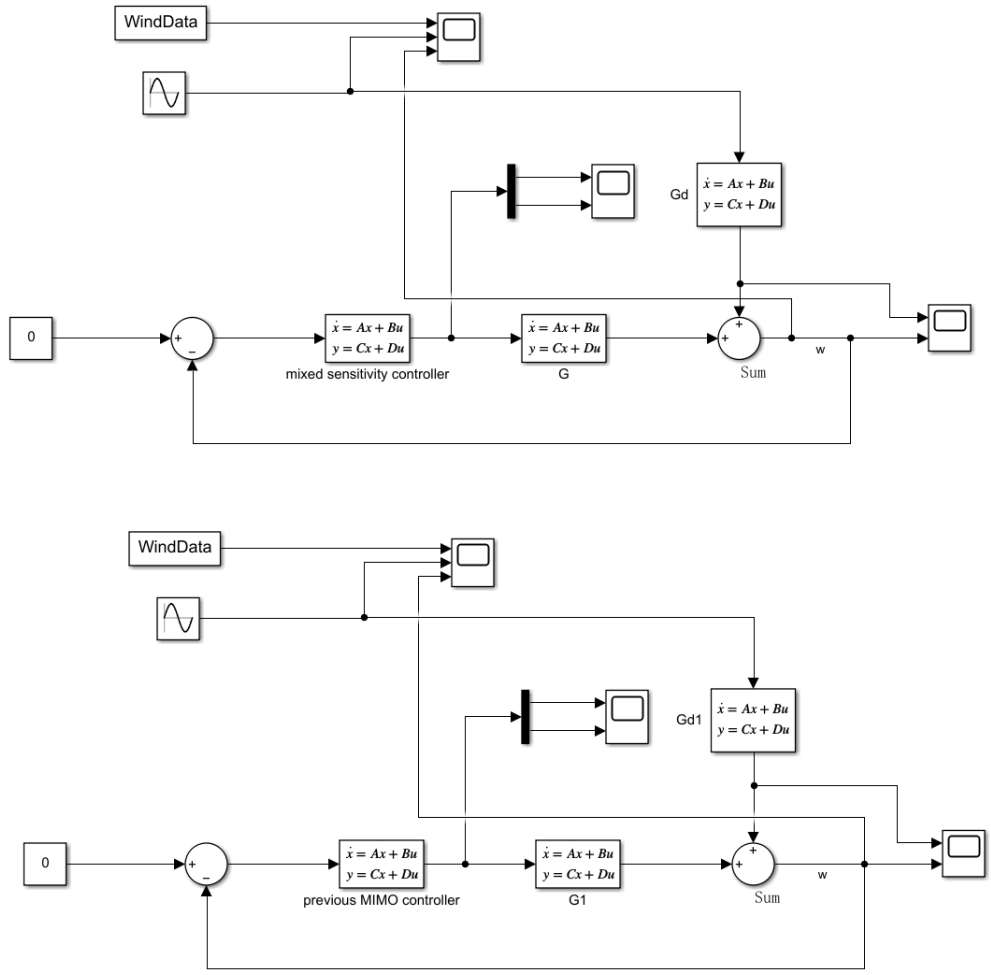

Figure 14: . Two systems with different controller: mixed-sensitivity controller and previous MIMO controller in simulink.

References

[1] Robust Control (SC42145). (2022, October 17). Retrieved from https://brightspace.tudelft.nl/d2l/le/content/501018/Home

[2] Multivariable Feedback Control. Siguird Skogestad and Ian Postlethwaite. Second edition. ISBN: 978-0-470-01168-3.

[3] Robust controller design using mu synthesis. MathWorks helping center. https://nl.mathworks.com/help/robust/ref.

[4] Options for musyn. MathWorks helping center. https://nl.mathworks.com/help/robust/ref/musynoptions.html

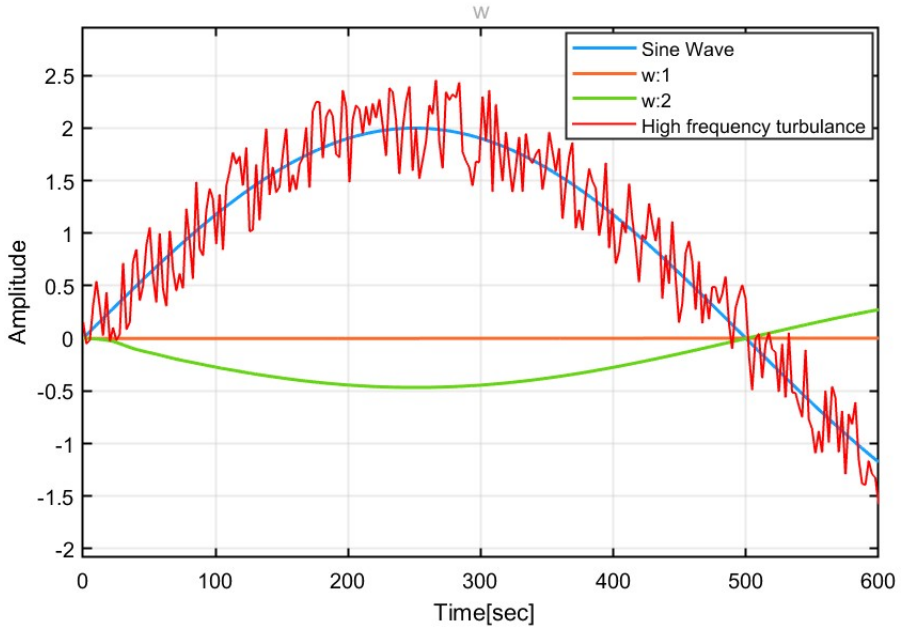

Figure 15: . Closed loop system's input and output with mixed-sensitivity controller.

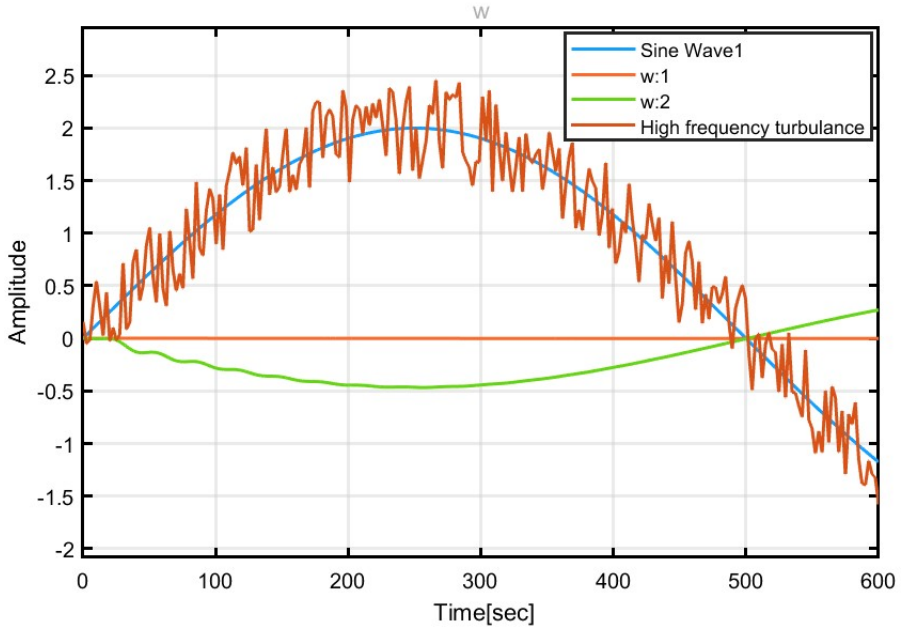

Figure 16: . Closed loop system's input and output with previous MIMO controller.

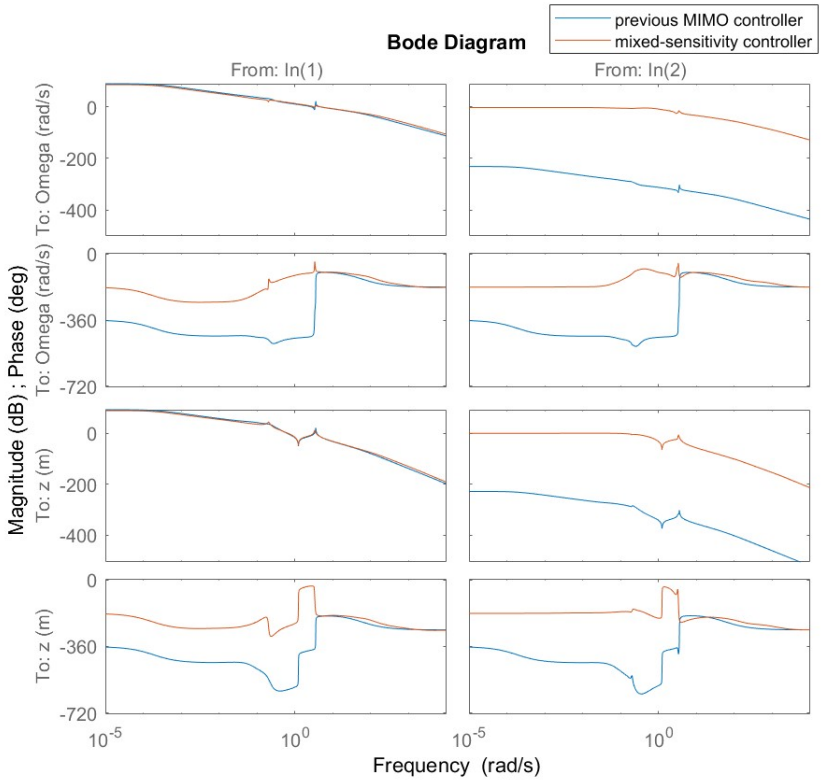

Figure 17: The bode plots of mixed-sensitivity controller and previous MIMO controller.

[5] H-infinity methods in control theory. Wikipedia. https://en.wikipedia.org/wiki